STOP-like protein 21 is a novel member of the STOP family, revealing a Golgi localization of STOP proteins.

Sylvie Gory-Fauré, Vanessa Windscheid, Christophe Bosc, Leticia Peris, Dominique Proietto, Ronald Franck, Eric Denarier, Didier Job, Annie Andrieux

STOP-LIKE PROTEIN 21: A NOVEL MEMBER OF THE STOP FAMILY REVEALING A GOLGI LOCALIZATION OF STOP PROTEINS

Sylvie Gory-Fauré‡, Vanessa Windscheid‡, Christophe Bosc‡, Leticia Peris‡, Dominique Proietto‡, Ronald Franck, Eric Denarier‡, Didier Job‡ and Annie Andrieux‡§**

Running Title: Golgi localization of STOP

From the ‡INSERM U366, DRDC/CS, CEA Grenoble, 17 rue des Martyrs, 38054 Grenoble cedex 9, France, ** AG Molecular Recognition, Gesellschaft für Biotechnologische Forschung, Mascheroder Weg 1, D-38124 Braunschweig, Germany

§ To whom correspondence should be addressed: INSERM U366, DRDC/CS, CEA Grenoble, 17 rue des Martyrs, 38054 Grenoble cedex 9, France. Tel: (33)-438-783-801; Fax: (33)-438-785-057; E-Mail: annie.andrieux@cea.fr.

Neuronal microtubules are stabilized by two calmodulin-regulated microtubule associated proteins, E-STOP and N-STOP, whose suppression in mice induces severe synaptic and behavioral deficits. Here we show that mature neurons also contain a 21 kD STOP-like protein, SL21, which shares calmodulin-binding and microtubule-stabilizing homology domains with STOP proteins. Accordingly, in different biochemical or cellular assays, SL21 has calmodulin-binding and microtubule-stabilizing activity. However, in cultured hippocampal neurons, SL21 antibodies principally stain the somatic Golgi and punctate Golgi material in neurites. In cycling cells, transfected SL21 decorates microtubules when expressed at high levels but is otherwise principally visible at the Golgi. The Golgi targeting of SL21 depends on the presence of cysteine residues located within the SL21 N-terminal domain, suggesting that Golgi targeting may require SL21 palmitoylation. Accordingly we find that SL21 is palmitoylated *in vivo*. N-STOP and E-STOP, which contain the Golgi targeting sequences present in SL21, also display distinct Golgi staining when expressed at low level in cycling cells. Thus neuronal proteins of the STOP family have capacity to associate with Golgi material, which could be important for STOP synaptic functions.

Neurons contain abundant sub-populations of stable microtubules that resist depolymerizing conditions such as exposure to the cold. This property is due to microtubule association with E-and N-STOP, two neuronal calmodulin-binding and calmodulin-regulated proteins (1-3). STOP proteins are important for synaptic function and STOP null mice present defects in both short- and long-term synaptic plasticity, associated with severe behavioral and neurotransmitter deficits (1,4). At the ultrastructural level, the main signature of STOP suppression is a dramatic depletion of synaptic vesicle pools in glutamatergic neurons.

E- and N-STOP arise from mRNA splicing of a single gene (5). These STOP proteins contain modular motifs (3) that are

either bi-functional (calmodulin-binding and microtubule-stabilizing sequences; Mc and Mn modules), or are comprised of calmodulin-binding sequences, unrelated to microtubule-stabilizing sequences.

We have previously described a number of STOP splicing variants, which are principally present in non-neuronal cells (6), but for a long time, STOPs seemed to be unique with no STOP-related proteins. However, strong evidence for a 21 kD STOP-like protein (SL21) has arisen from database searches (3). SL21 contains a 35 aa N-terminal stretch which shares 83% homology with the N-terminal part of E- or N-STOP, and contains a calmodulin-binding motif. A second domain of SL21, spanning 24 aa, shares 71% homology with a microtubule-stabilizing Mn module of E- and N-STOP (3,7).

Here, we demonstrate that SL21 is a neuronal protein, strictly expressed in the post-natal brain. We show that SL21 has microtubule-stabilizing activity similar to E- and N-STOP. However, surprisingly, endogenous SL21 co-localizes with the somatic Golgi apparatus and with dendritic Golgi structures in cultured hippocampal neurons. We show that the N-terminal part of SL21 comprises a Golgi-targeting sequence with critical cysteine residues, which sustain SL21 palmitoylation. The SL21 Golgi targeting sequence is also present and functional in E-and N-STOP.

In light of studies indicating that the presence of Golgi material in neurites and synapses may be important for synaptic plasticity (8), a Golgi interactions with STOP could be important for STOP function in synapses.

EXPERIMENTAL PROCEDURES

Sequence analysis - Mouse N-STOP protein sequence (GenBank Accession number CAA75930) was submitted to the BLAST program (http://www.ncbi.nlm.nih.gov/BLAST/) to identify STOP-related proteins. GenBank Accession numbers of these proteins were CAA63762 for rat N-STOP, NP_149052 for human N-STOP, XP_508647 for chimpanzee N-STOP, XP_596995 for cow N-STOP, NP_941001 for mouse SL21, XP_344040 for rat SL21, AAH06434 for human SL21, XP_516902 for chimpanzee SL21, and XP_608343 for cow SL21. Protein sequence alignments were performed using the multiple alignment software Clustal W (9).

Plasmid constructs - On the basis of the mouse SL21 cDNA sequence (GenBank Accession number BY727771), the entire open reading frame of mouse SL21 was amplified by PCR. We used Mouse Brain Marathon Ready cDNA (BD Biosciences) and the Advantage-GC2 Polymerase Mix (BD Biosciences), with primers containing Bgl II extensions. The resulting PCR product was first cloned into pCR2.1-TOPO (Invitrogen). For expression in mammalian cells, the complete coding sequence was cloned in pSG5 vector (Stratagene) and in pcDNA3.1(-)/Myc-His-A vector (Invitrogen) to be fused with the myc epitope DNA. For production and purification in bacterial system, the complete coding sequence was cloned into pGex-4T3 vector (Amersham Biosciences), to fuse GST after the last amino acids (aa) of SL21. The two SL21 deletion mutants were obtained by PCR, and correspond to Met + aa 35-191 (SL21Δ2-34) and to aa 1-122 + aa 146-191 (SL21ΔMn3), according to the numbering of mouse SL21 protein. The replacement of Cys5, Cys10 and Cys11 by glycine residues (SL21-C(5/10/11)G) was obtained by PCR, with a degenerate 5'- oligonucleotide (5'-AgA TCT ATg gCg Tgg CCC **ggC** ATC AgC Cgg CTA **ggC ggC** CTg gCC –3'). The STOP coding sequence of LNtΔMn1Mn2, corresponding to aa 1-123 + Ala + aa 139-161 + Ile-Gln + aa 175-225 according to the numbering of rat N-STOP, was amplified by PCR and then subcloned into the pcDNA3.1(-)/Myc-His-A vector to be fused with the myc epitope DNA. N-STOP plasmid is described in (2,10). The STOP coding sequence of N-STOPΔ2-19, corresponding to Met + aa 20-952 according to the numbering of rat N-STOP, was amplified by PCR and then subcloned into the pSG5 vector. All the SL21 and STOP constructs were confirmed by DNA sequencing.

Production of SL21-GST - Plasmid pGex-4T3 containing SL21 cDNA was transformed in One Shot BL21 (DEA3) Star cells (Invitrogen) according to the manufacturer's instructions. Transformed cells expressing SL21-GST were grown at 37° C to an OD_{600} of 0.6, and induced with 0.5 mM IPTG for 3 h at 37° C. Cells were pelleted and resuspended in PBS containing 1% Triton X-100, protease inhibitors (Complete Cocktail tablets, Roche) and sonicated for 1.5 min before centrifugation (17,000 *g* for 10 min). The supernatant was incubated with glutathione-Sepharose beads.

These beads were placed in columns and successively washed with PBS containing 1% Triton X-100, then with PBS and finally with 50 mM Tris, pH 8.0. The GST fusion proteins were eluted with 10 mM glutathione in 50 mM Tris (pH 8.0).

Western blot analysis - Tissues from mice were homogenized in a 100 mM K-Pipes, 1 mM EGTA, and 1 mM $MgCl_2$ buffer (pH 6.65). The homogenates were centrifuged at 200,000 *g* for 30 min at 4° C. Supernatants were then harvested and analyzed by SDS/PAGE (11). For immunoblotting, proteins were subsequently transferred onto nitrocellulose membranes and processed as previously described (12).

Sedimentation of proteins with microtubules - All proteins were pre-clarified at 150,000 *g* for 15 minutes in a TL-100 ultracentrifuge at 4°C prior start experiments. STOP proteins were purified as described in Pirollet et al (13). Microtubule-binding assay was performed as in Masson and Kreis (14) using taxol-stabilized microtubules (4 µM) as substrates and a 60% glycerol cushion.

Assay of Calmodulin Binding to Immobilized Peptide - Immobilized peptide arrays corresponding to the human SL21 were produced according to (15) with an ABIMED ASP 222 automated SPOT robot. The protein sequence was subdivided into 15-mer peptides with an overlap of 12 aa. The peptides were synthesized spotwise as an array on a specially manufactured cellulose membrane (AIMS Scientific Products GmbH, Braunschweig, Germany). The peptides are permanently linked to the membrane through their carboxy-terminal aa via a polyethylene glycol spacer. The synthesis procedure followed exactly that of (16). Overlay binding assay were performed as in (3), using [^{35}S]-labeled calmodulin.

Cell culture - Hippocampal cell cultures were prepared as previously described (17). Briefly, hippocampi brain tissue from E18.5 mice were removed and digested in 0.25% trypsin in Hepes-buffered Hanks' balanced salt solution (HBSS) at 37° C for 15 min. After manual dissociation, cells were plated at a concentration of 5,000–15,000 cells/cm^2 on poly-L-lysine (Sigma) coated coverslips, in DMEM - 10% FBS. One hour after plating, the medium was changed to DMEM containing B27 and N2 supplement (Invitrogen). HeLa and NIH 3T3 cells were cultured in RPMI-Glutamax or DMEM-Glutamax, respectively, supplement with 10% SVF and 1% penicillin/streptomycin (Invitrogen).

Transient Transfection and Analysis of microtubule Stability - Exponentially growing HeLa or NIH 3T3 cells were transfected with the cDNAs described above, using FuGENE 6 (Roche Diagnostics), according to the manufacturer's instructions. Transfected cells were either directly processed for immunofluorescence or exposed to cold temperature (30 min on ice) or to nocodazole (20 µM for 30 min). Cells were then permeabilized in lysis buffer (30 mM Pipes, 1 mM EGTA, 1 mM $MgCl_2$, 10% glycerol, 0.1% Triton X-100, pH 6.75) for 1 min, and processed for immunofluorescence.

Antibodies - Primary antibodies were: mAb against α-tubulin (TUB2.1) diluted to 1/100 (Sigma); rat mAb against tyrosinated tubulin (YL1/2) diluted to 1/5,000 (18); mAb against GM130 diluted to 1/50 and against GS28 diluted to 1/200 (BD Transduction Laboratories); rabbit polyclonal antibody against giantin (Covance) diluted to 1/2,000; rabbit polyclonal antibody 23C against STOP (2) diluted to 1/400. Rabbit polyclonal antibodies 3315, were raised against synthetic peptide FQVPEVRKFTPNPSAI, corresponding to aa 164-179 of mouse SL21 (Eurogentec). Serum 3315 was affinity-purified with the corresponding peptide and used diluted to 1/4,000 and to 1/400 for Western blot and immunofluorescence, respectively.

Secondary antibodies were: anti GST peroxydase-coupled (Santa Cruz); anti-mouse Alexa 488- (Molecular probes) or Cy5-coupled, anti-rabbit Cy3-coupled, and anti-rat Alexa 488-coupled (Jackson Immuno Research) antibodies.

Immunofluorescence - Hippocampal neurons were then either permeabilized in OPT buffer (80 mM Pipes, pH 6.7, 1 mM EGTA, 1 mM MgCl2, 0.5% Triton X-100, 10% glycerol) at 35°C for 2 min before fixation, or fixed directly for 10 min in methanol at -20°C. Cells were then incubated with primary antibodies for 45 min in PBS - Tween 0.5% and with secondary antibodies for 40 min. Cells were analyzed with a laser confocal microscope (TCS-SP2, Leica), or with an inverted microscope Axioscop 50 (Zeiss) controlled by Metaview (Universal Imaging, Downingtown, PA). Images were digitalized using a Coolsnap ES camera (Roper Scientific).

[^{3}H]-Palmitate labeling and Immunoprecipitation - HeLa cells were either non transfected or transfected with SL21-myc or SL21 C(5/10/11)G-myc cDNAs. One day after transfection, cells were labeled for 3 h with 500 µCi [^{3}H]-palmitic acid (Amersham). The radioactive palmitic acid was completely dried under nitrogen and resuspended in 12.5 µl of DMSO and complemented with 1 ml of RPMI containing 0,5% de-fatted BSA (Sigma). Cells were washed and scraped with PBS. After centrifugation at 12,000 *g* for 2 min cells were lysed in IP buffer (50 mM Tris, 150 mM NaCl, 0,05% deoxycholate, 1% Triton X-100, 10% glycerol, pH 8.0) in the presence of protease inhibitors (Complete Cocktail tablets, Roche) and 5 mM $CaCl_2$. After centrifugation of the cell lysate at 12,000 *g* for 5 min at 4° C, the supernatant was supplement with 5 mM EGTA and incubated for 2 h at 4° C with 25 µl myc antibody (Santa Cruz biotech) pre-incubated 2 hours at 4° C with 30 µl protein G-sepharose (Amersham). After centrigugation at 12,000 *g* for 2 min, immunoprecipitate were washed 5 times in IP buffer for 10 min at 4° C. Samples were separated by SDS-PAGE, and gels were fixed 30 min in 50% methanol - 10% acetic acid and treated 30 min with Amplify solution (Amersham), in order to improve the radioactive signal. The gels were dried and exposed on autoradiography films for 10 days at -80° C.

RESULTS

STOP homology domains in SL21 – E- and N-STOP contains two classes of bi-functional calmodulin-binding and stabilizing modules, Mc modules and Mn modules (Fig. 1A). E- and N-STOP also contains additional calmodulin-binding sequences unrelated to Mn or Mc modules (Fig. 1A). The first 35 aa of SL21 share 83% homology with the N-terminal aa of E- and N-STOP which comprises, in STOPs, the functional calmodulin-binding motif called Cam1 (3). A second domain of SL21, spanning 24 aa, share 71% homology with the E- and N-STOP bifunctional calmodulin-binding (Cam5) and microtubule-stabilizing Mn3 module (3). The homologous domains of N-STOP and SL21 are aligned figure 1B.

Calmodulin-binding properties of SL21 – All the STOP calmodulin-binding sites including Cam1 and Cam5 were initially identified as calmodulin-binding motifs on N-STOP immobilized peptide arrays (3). A similar assay with SL21 peptides (Fig. 2A-B) showed that the STOP Cam1 and Cam5 homologous motifs of SL21 (SL-Cam1 and SL-Cam3, respectively), also bound [^{35}S]-calmodulin (peaks 1 and 3, Fig. 2B-C), together with two other apparently weaker calmodulin-binding motifs, (SL-Cam2 and SL-Cam4, peaks 2 and 4 respectively) (Fig. 2B-C).

Calmodulin-binding motifs in N-STOP have been shown to bind to immobilized Ca^{2+}-calmodulin *in vitro* (3). Accordingly, 4 independents experiments consistently showed that recombinant SL21-GST bound to calmodulin column, as illustrated in Fig. 2D. The binding was strictly dependent on the presence of calcium as shown by the release of SL21 from the calmodulin column by EGTA buffer (Fig. 2D) and by the non-binding of SL21 to calmodulin column in the absence of calcium (Fig. 2D). The binding of SL21-GST to calmodulin is mediated by SL21 as GST alone was unable to bind to immobilized calmodulin (data not shown). Thus, SL21 behaves as a *bona fide* calmodulin-binding protein *in vitro*.

Microtubule-binding and stabilizing activity of SL21 – In E- and N-STOP, Mn modules mediate STOP association with microtubules with resulting inhibition of microtubule depolymerization upon exposure to the cold or to nocodazole (3). In agreement with the presence of a Mn module sequence in SL21, SL21 co-sedimented with taxol-stabilized microtubules in standard microtubule-binding assays, while remaining in the soluble fraction in the absence of microtubules (Fig. 3A). In the same microtubule-binding assay, N-STOP co-sedimented with microtubules whereas GST remained in the supernatant. In quantitative experiments, various amount of tubulin were polymerized and then incubated with GST-SL21 at 2 µM. Then, polymerized tubulin was pelleted and SL21 content was analyzed on immunoblots, in both supernatants and pellets (Figure 3B). The concentrations of tubulin at which approximately half of SL21 co-sedimented with microtubules was circa 5 µM (Figure 3B). In additional experiments, GST-SL21 at various concentrations was mixed with polymerized tubulin (10 µM). Then, microtubules were pelleted and SL21 content was analyzed on immunoblots, in both

supernatants and pellets (Figure 3C). In this experiment, SL21 at 4 μM was found both in the supernatant and in the pellet whereas at concentration of SL21, ranging from 2 μM to 0.5 μM, SL21 is only found associated with microtubules. Altogether these results showed that SL21 behaved as a microtubule-binding protein *in vitro*.

We used HeLa cells for microtubule-binding and -stabilization tests in *vivo*. HeLa cells are devoid of STOP, of SL21 and of cold-stable or nocodazole-resistant microtubules (Fig. 3D). When transfected in HeLa cells, a SL21 mutant (SL21Δ2-34), lacking the N-terminal domain and containing the Mn module, decorated cytoplasmic microtubules and induced both microtubule cold stability and microtubule resistance to nocodazole (Fig. 3E), compatible with functionality of the Mn module of SL21 *in vivo*. As shown below, the behavior of the full-length SL21 in cells was more complex than the mutant lacking the N-terminal domain (SL21Δ2-34), due to interfering influence of the N-terminal sequence.

Tissue distribution and cellular localization of endogenous SL21 - We used Western blot analysis of mouse tissues with SL21 polyclonal antibody 3315 to determine the distribution pattern of SL21. SL21 was only detected in brain tissue (Fig. 4A). In tissue extracts from new-born brain, SL21 expression was low at P0 and increased after P10 (Fig 4A). We then tested the presence of SL21 in various neuronal cell lines, using both immunoblot analysis and immunofluorescence microscopy. SL21 was not detected in neuronal cell lines (N2A, PC12 and NG108) whether cultured in the presence or absence of NGF (data not shown). In contrast, SL21 was present in neurons, in primary cultures, being absent from glial cells (data not shown). Interestingly, in differentiating hippocampal cultured neurons, SL21 antibodies principally stained a juxta-nuclear structure corresponding to the somatic Golgi apparatus, as demonstrated by co-localization with the cis-Golgi marker GS28 (Fig. 4B). At late stages of neuronal differentiation *in vitro* (16 DIV), in addition to the somatic Golgi, both SL21 and GS28 antibodies yielded a punctuated staining of neuritic extensions (Fig. 4B), corresponding to staining of neurite vesicular Golgi (19). A distinct microtubule staining was also visible after triton-soluble protein extraction (Figure 4D). Disruption of the somatic Golgi with Brefeldine A treatment, in differentiated neurons, induced a dramatic re-distribution of SL21 and GS28 stainings, which both became diffuse (Fig. 4C). These results indicate that SL21 is specifically expressed in differentiated neuronal cells and that it localizes to microtubules, to the somatic Golgi and to Golgi material traveling throughout neurites.

Dual localization of transfected SL21 in NIH 3T3 cells: *microtubule- and Golgi-targeting sequences in SL21*- We used NIH 3T3 cells which have a well organized somatic Golgi and SL21 mutants for further analysis of SL21 localization and domain structure. When expressed in NIH 3T3 cells, the apparent localization of SL21 varied as a function of its expression level. At low levels of expression, SL21 was principally detectable on the Golgi (Fig. 5A). At higher levels of expression, there was also distinct SL21 staining of cytoplasmic microtubules (Fig. 5B). The deletion of the Mn module (SL21ΔMn) suppressed the microtubule association of SL21, at all expression levels, while preserving Golgi localization (Fig. 5C). Conversely, at all levels of expression in NIH 3T3 cells, a deletion mutant of SL21 lacking 34 N-terminal aa (SL21Δ2-34), associated with microtubules (data not shown) as in the case of HeLa cells (Fig. 3F) with no Golgi localization. In additional microtubule stabilization assays in HeLa cells, we found that native SL21 expressed at high levels and the SL21Δ2-34 deletion mutant had microtubule stabilizing activity, whereas the SL21 mutant SL21ΔMn, which shows exclusive Golgi localization, had no detectable effect on microtubule stability (not shown).

Altogether, these results indicate that the targeting of SL21 to microtubules depends on the presence of the Mn module and that SL21 comprises a Golgi-targeting sequence located in the N-terminal domain of the protein.

Palmitoylation of SL21 - Palmitoylation is often required for protein association with membranes and has been previously observed in neuronal proteins associated with tubulin and with the Golgi such as SCG10 (20). Palmitoylation occurs at cysteine residues surrounded with basic residues (21). Mouse

SL21 contains 3 cysteine residues, all located in the Golgi-targeting domain (positions 5, 10 and 11) and surrounded by basic residues (Fig. 6A). To assess whether these cysteines were involved in the localization of SL21 to the Golgi apparatus, we produced cDNAs encoding SL21 mutants in which Cys5, Cys10 and Cys11 were replaced by glycine residues. These constructs were then transfected in NIH 3T3 cells, and the Golgi localization of the mutants was examined. In contrast to SL21, which localizes to the Golgi, the SL21 mutant where all the three cysteine residues were replaced (SL21-C(5/10/11)G) did not localize to the Golgi, but co-localized with microtubules (Fig. 5D). These results indicate a requirement of SL21 N-terminal Cys5, Cys10, Cys11 for proper localization of SL21 to Golgi apparatus. To test SL21 palmitoylation directly, HeLa cells were incubated with [^{3}H]-palmitate, with or without prior transfection with SL21-myc or SL21-C(5/10/11)G-myc cDNA. Then, SL21-myc and SL21-C(5/10/11)G-myc were immunoprecipitated from cell extracts and the immunoprecipitated proteins were analyzed both by Western blot, using SL21 polyclonal antibody 3315, and by autoradiography (Fig. 5E). As shown in Fig. 5E, SL21 incorporated ^{3}H, whereas SL21-C(5/10/11)G mutant did not, demonstrating that SL21 is indeed palmitoylated in cells and showing the crucial role of Cys5, Cys10 and Cys 11 in this process. These results were obtained for 3 independent experiments and similar results were observed when using SL21-GFP instead of SL21-myc (data not shown).

Golgi targeting of N-STOP - The N-terminal Golgi-targeting sequence of SL21, which is conserved among mammals, is also present at the N-terminus of N-STOP (Fig. 6A). Accordingly, a 225 aa N-terminal fragment of N-STOP containing the Golgi-targeting sequence and deleted for microtubule binding modules, Mn1 and Mn2 (LNtΔMn1Mn2) was uniformly addressed to the Golgi when transfected in NIH3T3 cells (Fig 6B). Despite the presence of such a functional Golgi-targeting sequence at their N-terminus, E- and N-STOP have not been detected at the Golgi in previous studies, this could be due either to a dominant influence of the STOP microtubule-targeting sequences (Mn and Mc modules) or to unfavorable experimental procedures. To test these possibilities, we re-examined N-STOP localization in various cell types and conditions. In neurons, STOP antibody yielded a bright staining of the whole cell body, making a possible STOP localization at the Golgi hard to detect (2).Interestingly, in NIH 3T3 cells, transfected N-STOP staining was principally detectable at the Golgi at low levels of expression (Fig. 6C) both Golgi and microtubule staining being present at high expression levels (Fig. 6D). Moreover, a transfected N-STOP mutant (N-STOPΔ2-19), lacking the Golgi targeting sequence, failed to associate with the Golgi (Fig. 6E). Altogether, these results indicate that the ability to localize to Golgi material is a shared property of STOP and STOP-like proteins, due to the presence of a Golgi-targeting sequence in their shared N-terminal domain.

DISCUSSION

In this study, SL21 and neuronal STOPs (E-STOP and N-STOP) emerge as a class of microtubule-binding and calmodulin-binding proteins, sharing both a Golgi-targeting sequence and microtubule-stabilizing modules. We note that the STOP Golgi-targeting sequence is only present in E-and N-STOP being absent from all the other known STOP variants (6). As E- and N-STOP, SL21 is specific of neurons and both SL21 and N-STOP are expressed only in the post-natal brain. Despite such similarities in structure and activity, there is an apparent difference in the cellular distribution of endogenous SL21 and N-STOP, SL21 being preferentially associated with the somatic Golgi and N-STOP with microtubules, in neurons. However both SL21 and N-STOP are principally detected at the Golgi when expressed at low levels in cells, whereas being also visible on cytoplasmic microtubules at high levels of expression. The apparent differences between endogenous SL21 and N-STOP localization in neurons may thus reflect differences in expression levels, N-STOP probably being much more abundant than SL21. Superimposed cell regulations may also affect SL21 or STOP localization. The Golgi targeting of SL21 and of STOP most likely depend on palmitoylation, which is a regulated and reversible covalent protein modification (22,23). Also, the microtubule-binding activity of Mn modules can be inhibited by calmodulin (24) and, in the case of STOP, through phosphorylation, opening the

possibility of a protein shift from microtubules to other cell compartments (25).

Why should neurons contain specific microtubule-associated proteins with Golgi-binding activity? The somatic Golgi in neurons has an organization similar to that observed in non-neuronal cells, although the Golgi orients toward the longest dendrite and this Golgi polarity precedes the asymmetric dendrite growth (26). Additionally there is evidence for the presence of Golgi material along neurites. Previous ultrastructural studies have reported membranes analogous to Golgi cisternae within the spines of distal dendrites (27,28). Moreover many neurons possess both somatic Golgi and discrete, discontinuous Golgi-type structures ("Golgi outposts") located far into the dendrites. These "Golgi outposts" are mobiles structures and are positioned to serve particular dendrites regions or sets of synapses, where they may be important for synaptic plasticity (8,19). Ability of Golgi binding may therefore be important for the function of N-STOP in synaptic plasticity (1). Additionally, palmitoylation may allow STOP interaction with vesicular or membrane material other than the Golgi (29) and may thereby be central for the dramatic effects of STOP suppression on the synaptic vesicle density (1). Moreover, palmitoylation has specifically been shown to play a role in neuronal protein trafficking, and in the clustering of receptors and the associated scaffolding proteins at synapses (29,30).

According to the present study, SL21 and STOP have extensively overlapping activities. Yet, STOP suppression is not compensated by SL21 in STOP deficient mice and we have not detected any obvious modification in SL21 expression (data not shown). What is the utility of SL21 in the presence of STOP? We have performed SL21 siRNA experiments in hippocampal neurons, with inconclusive results (data not shown). It is likely that, as for N-STOP, SL21 function will be revealed by its suppression in whole animals, where complex aspects of synaptic function can be investigated. STOP or SL21 null animals may offer exciting models to test a role of the Golgi in integrated brain functions.

REFERENCES

1. Andrieux, A., Salin, P. A., Vernet, M., Kujala, P., Baratier, J., Gory-Fauré, S., Bosc, C., Pointu, H., Proietto, D., Schweitzer, A., Denarier, E., Klumperman, J., and Job, D. (2002) *Genes Dev* **16**(18), 2350-2364
2. Guillaud, L., Bosc, C., Fourest-Lieuvin, A., Denarier, E., Pirollet, F., Lafanechère, L., and Job, D. (1998) *J Cell Biol* **142**(1), 167-179
3. Bosc, C., Frank, R., Denarier, E., Ronjat, M., Schweitzer, A., Wehland, J., and Job, D. (2001) *J Biol Chem* **276**(33), 30904-30913
4. Brun, P., Bégou, M., Andrieux, A., Mouly-Badina, L., Clerget, M., Schweitzer, A., Scarna, H., Renaud, B., Job, D., and Suaud-Chagny, M. F. (2005) *J Neurochem* **94**(1), 63-73
5. Denarier, E., Aguezzoul, M., Jolly, C., Vourc'h, C., Roure, A., Andrieux, A., Bosc, C., and Job, D. (1998) *Biochem Biophys Res Commun* **243**(3), 791-796
6. Galiano, M. R., Bosc, C., Schweitzer, A., Andrieux, A., Job, D., and Hallak, M. E. (2004) *J Neurosci Res* **78**(3), 329-337
7. Bosc, C., Andrieux, A., and Job, D. (2003) *Biochemistry* **42**(42), 12125-12132
8. Horton, A. C., and Ehlers, M. D. (2004) *Nat Cell Biol* **6**(7), 585-591
9. Thompson, J. D., Higgins, D. G., and Gibson, T. J. (1994) *Nucleic Acids Res* **22**(22), 4673-4680
10. Bosc, C., Cronk, J. D., Pirollet, F., Watterson, D. M., Haiech, J., Job, D., and Margolis, R. L. (1996) *Proc Natl Acad Sci U S A* **93**(5), 2125-2130
11. Laemmli, U. K. (1970) *Nature* **227**(259), 680-685
12. Lieuvin, A., Labbé, J. C., Dorée, M., and Job, D. (1994) *J Cell Biol* **124**(6), 985-996
13. Pirollet, F., Derancourt, J., Haiech, J., Job, D., and Margolis, R. L. (1992) *Biochemistry* **31**(37), 8849-8855

14. Masson, D., and Kreis, T. E. (1993) *J Cell Biol* **123**(2), 357-371
15. Frank, R. (1992) *Tetrahedron* **48**, 9217-9232
16. Frank, R., and Overwin, H. (1996) *Methods Mol Biol* **66**, 149-169
17. Dotti, C. G., Sullivan, C. A., and Banker, G. A. (1988) *J Neurosci* **8**(4), 1454-1468
18. Wehland, J., and Willingham, M. C. (1983) *J Cell Biol* **97**(5 Pt 1), 1476-1490
19. Horton, A. C., and Ehlers, M. D. (2003) *J Neurosci* **23**(15), 6188-6199
20. Di Paolo, G., Lutjens, R., Pellier, V., Stimpson, S. A., Beuchat, M. H., Catsicas, S., and Grenningloh, G. (1997) *J Biol Chem* **272**(8), 5175-5182
21. Resh, M. D. (1999) *Biochim Biophys Acta* **1451**(1), 1-16
22. Ross, E. M. (1995) *Curr Biol* **5**(2), 107-109
23. Mumby, S. M. (1997) *Curr Opin Cell Biol* **9**(2), 148-154
24. Job, D., Fischer, E. H., and Margolis, R. L. (1981) *Proc Natl Acad Sci U S A* **78**(8), 4679-4682
25. Baratier, J., Peris, L., Brocard, J., Gory-Faure, S., Dufour, F., Bosc, C., Fourest-Lieuvin, A., Blanchoin, L., Salin, P., Job, D., and Andrieux, A. (2006) *J Biol Chem*
26. Horton, A. C., Racz, B., Monson, E. E., Lin, A. L., Weinberg, R. J., and Ehlers, M. D. (2005) *Neuron* **48**(5), 757-771
27. Pierce, J. P., van Leyen, K., and McCarthy, J. B. (2000) *Nat Neurosci* **3**(4), 311-313
28. Pierce, J. P., Mayer, T., and McCarthy, J. B. (2001) *Curr Biol* **11**(5), 351-355
29. el-Husseini Ael, D., and Bredt, D. S. (2002) *Nat Rev Neurosci* **3**(10), 791-802
30. Huang, K., and El-Husseini, A. (2005) *Curr Opin Neurobiol* **15**(5), 527-535

FOOTNOTES

* We thank A. Schweitzer and N. Collomb for their technical assistance; Y. Saoudi for help in imaging; Julien Fauré, Jacques Brocard and J.C. Deloulme for their helpful discussions. This work was supported in part by grants from La Ligue Nationale contre le Cancer to D.J.

The abbreviations used are: SL21, STOP-Like of 21 kD; STOP, Stable Tubule Only Polypeptide; aa, amino acids; MAP, microtubule-associated protein

FIGURE LEGENDS

Figure 1: STOPs and SL21 conserved domains

(A) Schematic representations of mouse N-STOP, E-STOP and SL21. Calmodulin-binding sites (*asterisks*) and microtubule-stabilizing modules Mn and Mc (green and dark gray, respectively) are represented on E- and N-STOP. Calmodulin-binding sites Cam1 and Cam5 and aa numbering are indicated. N-STOP C-terminal repeats, absent in E-STOP, are in light gray. The common N-terminal

domain is in yellow. (B) Alignment of SL21 and STOP conserved N-terminal sequences (top) and of conserved Mn module (bottom). Conserved amino acids are shown in red. The N-STOP calmodulin-binding sequences Cam1 and Cam5 are underlined. Numbers correspond to aa position in mouse SL21 and N-STOP proteins.

Figure 2: Calmodulin-binding properties of SL21

Identification of SL21 calmodulin-binding motifs using immobilized peptide array and calmodulin-agarose binding of SL21. (A) [^{35}S]-labeled calmodulin overlay of a membrane containing SL21 immobilized peptide array. The overlapping peptides (15-mers, with an orverlap of 12 aa) were numbered from the amino-terminal to the carboxyl-terminal residues of SL21. Numbers correspond to the first peptide of each line. Four peptide clusters interacting with [^{35}S]-labeled calmodulin were detected by autoradiography. (B) Quantitative analysis of [^{35}S]-calmodulin binding to mouse SL21 peptides. The radioactive signals observed in A were quantified using phosphorimager and results were plotted. Signal values are in arbitrary units (A. U.). The four peaks of maximum radioactivity signal correspond to SL21 aa 6-20 (peak 1), aa 87-101 (peak 2) aa 141-155 (peak 3) aa 177-191 (peak 4). (C) Calmodulin-binding sites SLCam1 to SLCam4, corresponding to peaks 1 to 4 in (B), are reported on the schematic representation of SL21 (asterisks) and their sequences are given. (D) Binding of SL21-GST to immobilized calmodulin-agarose. Recombinant SL21-GST was produced in bacteria and loaded onto a calmodulin-agarose column in the presence (left panel) or in the absence (right panel) of 1 mM Ca^{2+}. The column was washed and proteins were subsequently eluted with EGTA-containing buffer. Equal aliquots of the loaded sample (L), flow-through fraction (F), and EGTA elution fractions (1-5) were analyzed for SL21-GST content using SDS-PAGE gel electrophoresis followed by immunoblot analysis with SL21 polyclonal antibody 3315.

Figure 3: Microtubule-binding and -stabilizing activity of SL21

(A-C) Microtubules co-sedimentation assays. (A) Co sedimentation of SL21-GST, N-STOP and GST with taxol-stabilized microtubules (10μM). SL21-GST, N-STOP and GST were incubated with (+) or without (-) taxol-stabilized microtubules (MT). The samples were then sedimented through a 60% glycerol

cushion. The supernatants (S) and the pellets (P) were analyzed for SL21, N-STOP and GST content by immunoblot using SL21 polyclonal antibody 3315, N-STOP polyclonal antibody 23C and GST antibody, respectively. (B) Various amount of tubulin (3 µM, 13 µM, 26µM and 40 µM) were polymerized, mixed with GST-SL21 (2 µM) and centrifuged. Equal amounts of supernatant and pellets were separated by SDS PAGE and were stained with Commassie blue, showing no detectable amount of tubulin in the supernatant. The supernatants (S) and the pellets (P) were analyzed for SL21 content by immunoblot using SL21 polyclonal antibody 3315. (C) Various amount of SL21 (4 µM, 2 µM, 1 µM and 0.5 µM) were incubated with polymerized tubulin (10µM). After centrifugation, equal amount of supernatants and pellets were separated by SDS PAGE and analyzed for SL21 content by immunoblot using SL21 polyclonal antibody 3315.

(D-E) Microtubules stability in cells. HeLa cells were either non-transfected (D) or transfected with a cDNA encoding SL21 mutant lacking the N-terminal domain and containing the Mn module (SL21Δ2-34) (E). After 24 h, cells were either maintained at 37° C, exposed to 4° C, or treated with 20µM nocodazole for 30 min. Cells were then double-stained for microtubules (α-tubulin mAb) and for SL21Δ2-34 (SL21 polyclonal antibody 3315). Bar, 10 µm.

Figure 4: Tissue distribution and cellular localization of SL21.

(A) Immunoblot analysis of adult mouse tissues and post-natal brain (P0-P10) using SL21 polyclonal antibody 3315. (B) Distribution of SL21 protein in cultured mouse hippocampal neurons, after 9 or 16 days of differentiation *in vitro* (DIV). Double staining of SL21 and Golgi was performed using SL21 polyclonal antibody 3315 and GS28 monoclonal antibody. Images were acquired using laser confocal microscopy. Bar, 40 µm. (C) Golgi-dependent localization of SL21. Hippocampal neurons, after 9 DIV were either untreated or treated with Brefeldine A (10 µg/ml) for 1 h or 4 h. SL21 and Golgi stainings and image acquisition were as in (B). (D) Distribution of SL21 protein in cultured mouse hippocampal neurons (9 DIV) after permeabilisation of the cells. Triple staining of SL21, microtubules and Golgi was performed using SL21 polyclonal antibody 3315, anti α tubulin and GS28 monoclonal antibodies. After triton-soluble protein extraction, SL21 staining can be observed on microtubule network. Bar, 8 µm.

Figure 5: Golgi versus microtubule localization of SL21 and SL21 mutants in transfected cells.

(A-B) NIH 3T3 cells transfected with a cDNA encoding the complete form of SL21. Double immunofluorescence analysis was performed using an SL21 polyclonal antibody 3315 and either GM130 mAb for Golgi staining (A) or α-tubulin mAb for microtubule staining (B). Cells were expressing either low (A) or high levels (B) of SL21. All the image acquisitions and merges were performed using laser confocal microscopy. (C) NIH 3T3 cells transfected with a cDNA encoding SL21ΔMn and double-stained for Golgi (GM130 mAb) and for SL21ΔMn (SL21 polyclonal antibody 3315). (D) NIH 3T3 cells transfected with a cDNA encoding SL21-C(5/10/11)G and triple stained for microtubules (YL1/2 mAb), Golgi (GM130 mAb) and SL21 (SL21 polyclonal antibody 3315). Bar, 20 μm (A, C, D) and 16 μm (B). Schematic representations of proteins are as in Fig. 1A. (E) Incorporation of [^{3}H]-palmitate into SL21-myc and SL21-C(5/10/11)G-myc mutant. HeLa cells overexpressing SL21-myc or SL21-C(5/10/11)G-myc mutant were incubated with [^{3}H]-palmitate, and proteins were immunoprecipited with anti myc antibody. Immunoprecipited proteins were separated by SDS-PAGE and subject to autoradiography or Western blot using SL21 polyclonal antibody 3315. Untransfected cells were used as control.

Fig. 6. Golgi-targeting of the N-terminal domain of N-STOP.

(A) Alignment of the N-terminal domains of STOP and SL21 proteins from various species, as indicated. Amino acids conserved in N-STOP and SL21 are boxed in black. Among the strongly conserved aa, the cysteine residues 5, 10 and 11 are boxed in red. Numbers correspond to aa position. (B) NIH 3T3 cells transfected with a cDNA encoding STOP fragment LNtΔMn1Mn2-myc and double-stained for Golgi (Giantin polyclonal antibody) and for LNtΔMn1Mn2 (myc mAb). (C-D) NIH 3T3 cells transfected with a cDNA encoding N-STOP and expressing either low (C) or high levels (D) of N-STOP. Cells were double-stained for STOP (polyclonal antibody 23C) and either for Golgi (GM130 mAb) or microtubule (α-tubulin mAb). (E) NIH 3T3 cells transfected with a cDNA encoding N-STOPΔ2-19 and double-stained for STOP (polyclonal antibody 23C) and for microtubule (α-tubulin mAb). Schematic representations of proteins are as in Fig. 1A. Bar, 20 μm.

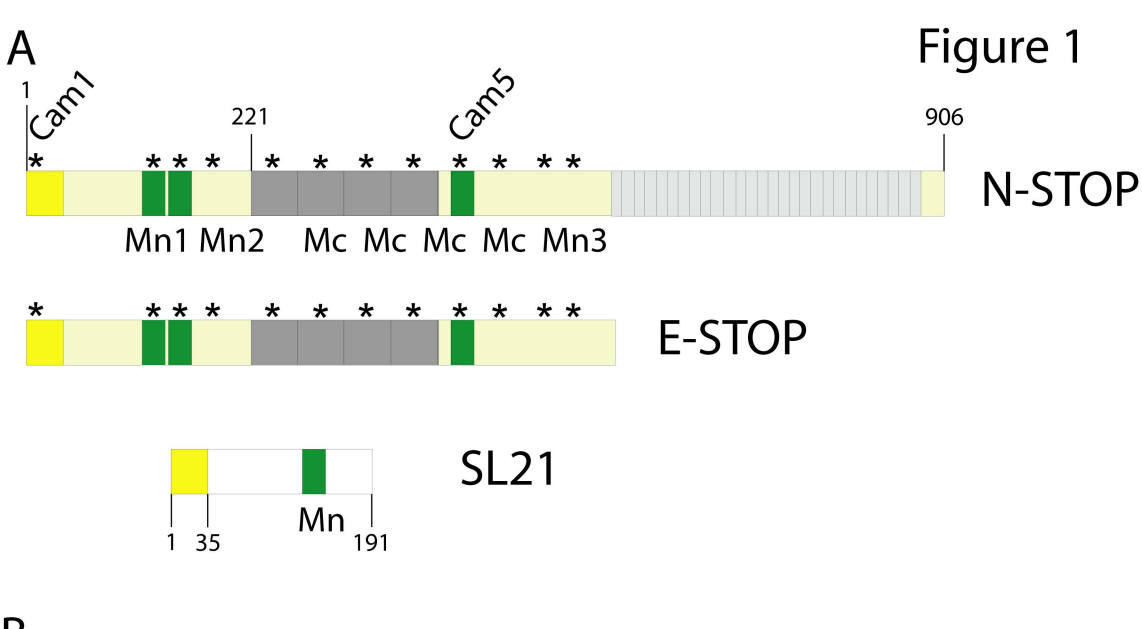

B

	1	35
SL21 N-ter	MAWPCISRLCCLARRWNQLDRSDVAVPLTLHGYSD	
STOP N-ter	MAWPCITRACCIARFWNQLDKADIAVPLVFTKYSE	
	1	35

	123	146
SL21 Mn module	TTSYRQEFQAWTGVKPSRSTKART	
STOP Mn3 module	SSSYRNEFRAWTDIKPVKPIKAKP	
	427	450

Figure 2

A

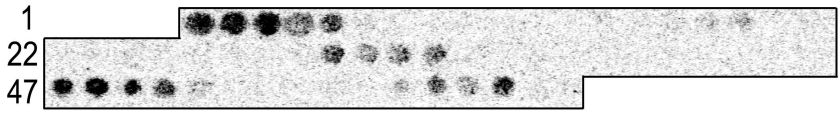

B

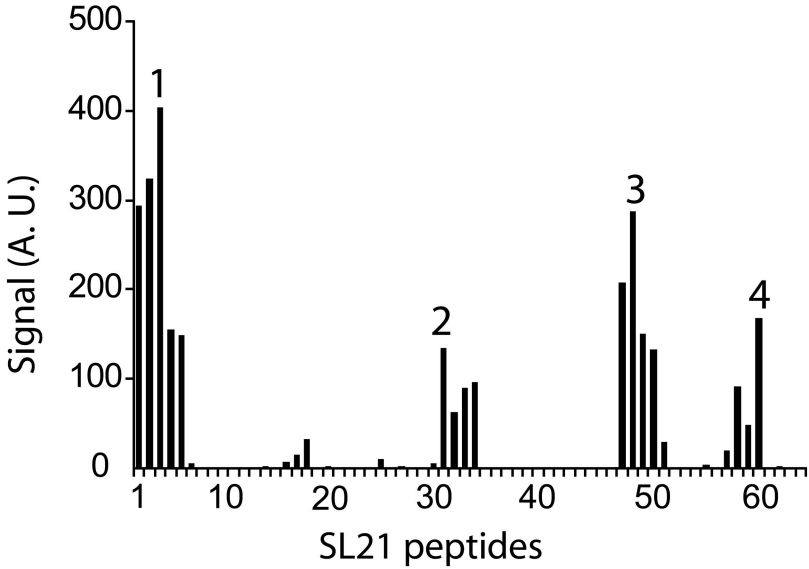

C

Peptide	Sequence
SLCam1	ISRLCCLARRWNQLD
SLCam2	PGRGPGAGGRRGKSS
SLCam3	TGVKPSRSTKTKPAR
SLCam4	VRKKFTPNPSAIFQA

D

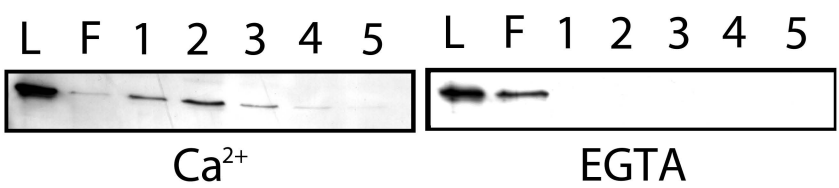

Figure 3

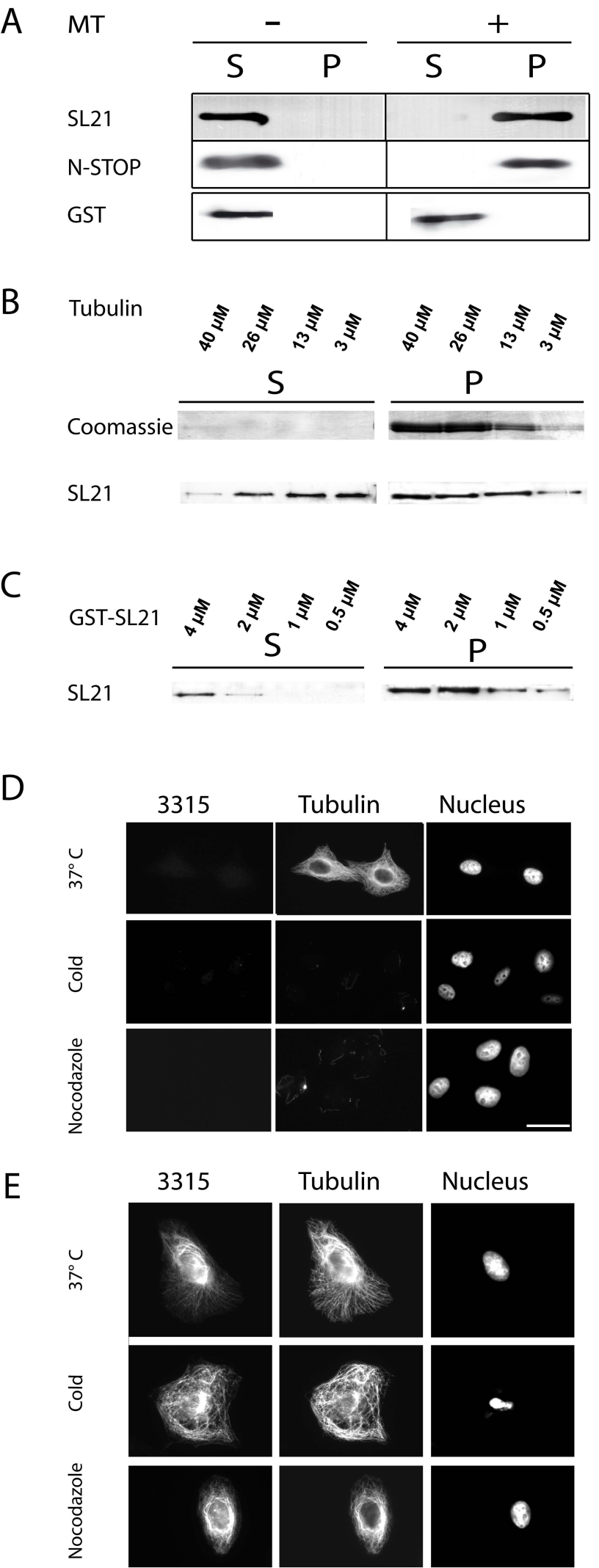
A
MT
–
+
S
P
S
P
SL21
N-STOP
GST
B
Tubulin
40 µM
26 µM
13 µM
3 µM
40 µM
26 µM
13 µM
3 µM
S
P
Coomassie
SL21
C
GST-SL21
4 µM
2 µM
1 µM
0.5 µM
4 µM
2 µM
1 µM
0.5 µM
S
P
SL21
D
3315
Tubulin
Nucleus
37° C
Cold
Nocodazole
E
3315
Tubulin
Nucleus
37° C
Cold
Nocodazole

Figure 4

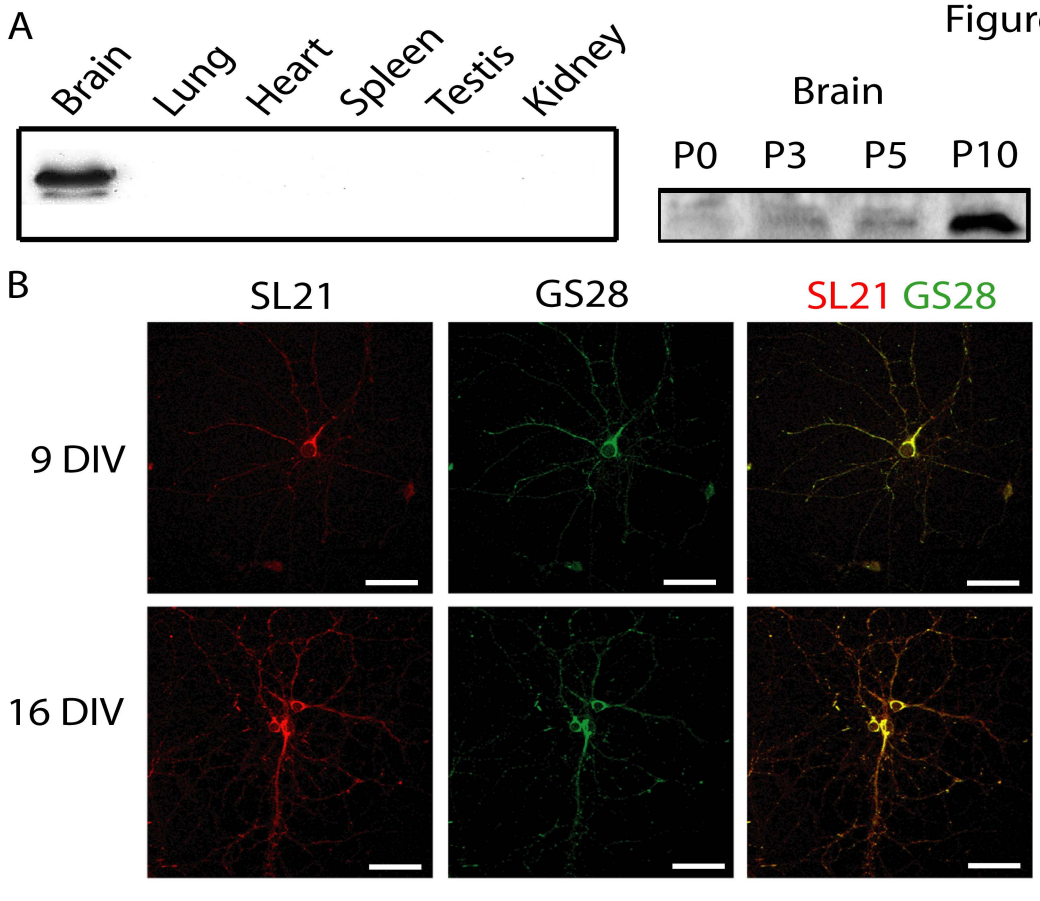
A
Brain
Lung
Heart
Spleen
Testis
Kidney
Brain
P0
P3
P5
P10
B
SL21
GS28
SL21 GS28
9 DIV
16 DIV
C
no BFA
1 h BFA
4 h BFA
GS28
SL21
D
SL21
GS28
tubulin
SL21 tubulin
Control
Permeabilized

Figure 5

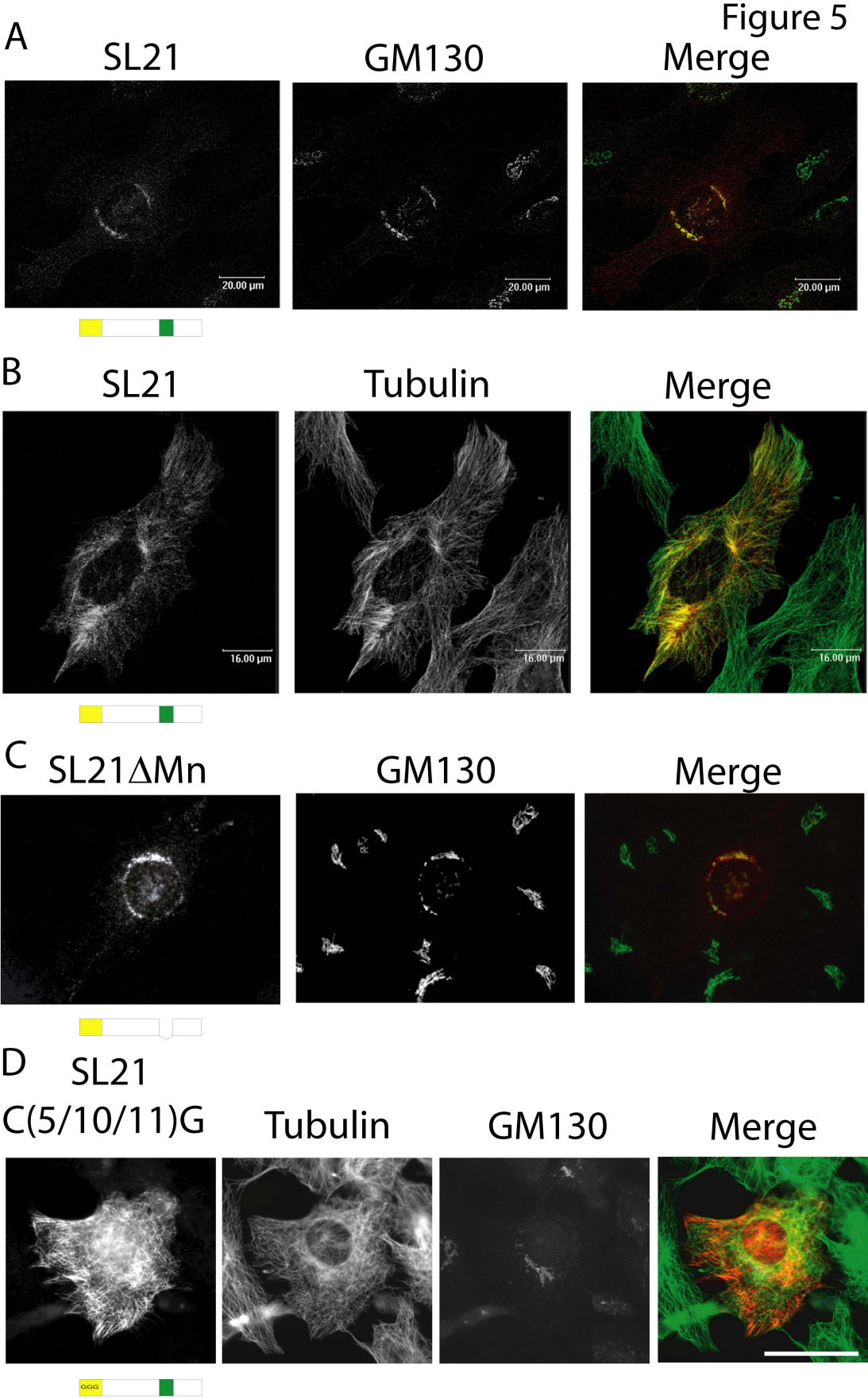
A
SL21
GM130
Merge
20.00 µm
20.00 µm
20.00 µm
B
SL21
Tubulin
Merge
16.00 µm
16.00 µm
16.00 µm
C
SL21ΔMn
GM130
Merge
D
SL21
C(5/10/11)G
Tubulin
GM130
Merge
E
Control
SL21
SL21
C(5/10/11)G
[3H]-palmitate
3315

Figure 6

A

B

C

D

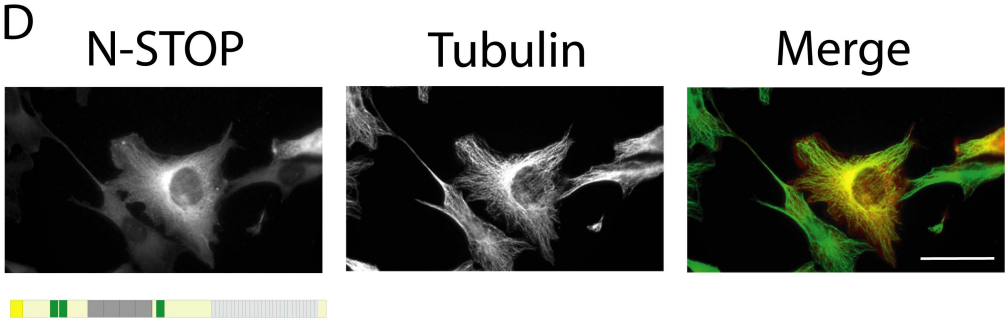

E